*Protein Science* (2000), *9*:2059–2067. Cambridge University Press. Printed in the USA.


# Solution structure of HpTX2, a toxin from *Heteropoda venatoria* spider that blocks Kv4.2 potassium channel

CÉDRIC BERNARD,[1] CHRISTIAN LEGROS,[2] GILLES FERRAT,[1] ULRIKE BISCHOFF,[3] ANNETTE MARQUARDT,[2] OLAF PONGS,[2] AND HERVÉ DARBON[1]

[1]AFMB, CNRS UMR 6098, IFR1, 31, Chemin Joseph-Aiguier, 13402 Marseille Cedex 20, France
[2]Institut für Neurale Signalverarbeitung, ZMNH, Universität Hamburg, Martinistr. 52, D-20246 Hamburg, Germany
[3]GENIONmbH, Absteistr. 57, D-20149 Hamburg, Germany

(RECEIVED April 12, 2000; FINAL REVISION June 19, 2000; ACCEPTED June 30, 2000)

**Abstract**

HpTX2 is a toxin from the venom of *Heteropoda venatoria* spider that has been demonstrated to bind on Kv4.2 potassium channel. We have determined the solution structure of recombinant HpTX2 by use of conventional two-dimensional NMR techniques followed by distance-geometry and molecular dynamics. The calculated structure belongs to the Inhibitory Cystin Knot structural family that consists in a compact disulfide-bonded core, from which four loops emerge. A poorly defined two-stranded antiparallel $\beta$-sheet (residues 20–23 and 25–28) is detected. Analysis of the electrostatic charge anisotropy allows us to propose a functional map of HpTX2 different from the one described for $\kappa$-conotoxin PVIIA, but strongly related to the one of charybdotoxin. The orientation of the dipole moment of HpTX2 emerges through K27 which could therefore be the critical lysine residue. Close to this lysine are a second basic residue, R23, an aromatic cluster (F7, W25, W30) and an hydrophobic side chain (L24). The high density in aromatic side chains of the putative functional surface as well as the lack of an asparagine is proposed to be the structural basis of the specificity of HpTX2 toward Kv4.2 channel.

**Keywords:** heteropodatoxin; NMR; spider toxin; structure determination; voltage-dependent potassium channel

Numerous peptidic toxins acting as potassium channel blockers have been identified in scorpion toxins. They all are small (29 to 39 amino acid residues), highly structured thanks to three (rarely four) disulfide bridges (Possani, 1984; Miller, 1995). They are structurally organized around a common structural motif named Cs$\alpha\beta$ (cystine stabilized alpha/beta motif) and their three-dimensional (3D) structure comprises a short alpha-helix and a double- or a triple-stranded antiparallel $\beta$-sheet (for a review, see Darbon et al., 2000). They interact with their receptor via the solvent-exposed surface of the $\alpha$-helix if the target is a small conductance calcium-activated potassium channel or via the solvent-exposed surface of the $\beta$-sheet if their target is a large conductance calcium-activated potassium channel or a voltage-dependent potassium channel (Darbon et al., 2000). Whatever their specificities are, their functional sites are made of a solvent exposed surface, rich in basic residues. We have previously proposed that the electrostatic anisotropy present in all these proteins was responsible for the correct orientation of the peptidic inhibitor with respect to its target (Blanc et al., 1997; Fremont et al., 1997; Renisio et al., 1999, 2000). The functional surface of Kv channel inhibitors comprises a triplet of residues (lysine, methionine/isoleucine, asparagine) (Goldstein et al., 1994; Aiyar et al., 1996; Naranjo & Miller, 1996; Rangananthan et al., 1996) associated with a doublet of basic residues and an aromatic residue (Goldstein et al., 1994; Rangananthan et al., 1996).

Another peptidic inhibitor of potassium channels, apamin, has been purified from the bee venom. Despite a strong difference in its 3D organization (a short $\alpha$-helix but no $\beta$-sheet in this 18 residues peptide) (Bystrov et al., 1980; Pease & Wemmer, 1988), it also presents the same kind of anisotropy, therefore interacting with small conductance calcium-activated potassium channel via its solvent-exposed, highly basic $\alpha$-helix surface (Vincent et al., 1975; Habermann & Fischer, 1979).

Another type of structural organization, namely Inhibitor Cystine Knot (ICK), motif, which consists in a compact disulfide-bonded core from which several short loops emerge (Wakamatsu et al., 1992), has been described for ion channel peptidic inhibitors, blockers of sodium channels (Hill et al., 1997), or calcium channels (Flinn et al., 1999), but only once for blockers of potassium channels (Scanlon et al., 1997). In this paper, we describe the solution structure, obtained by two-dimensional-$^1$H-NMR techniques, of HpTX2 toxin from *Heteropoda venatoria* spider venom,

Reprint requests to: Herve Darbon, AFMB-UPR 9030, CNRS IFR1, 31 Chemin Joseph-Aiguier, Marseille Cedex, 13402 France; e-mail: herve@afmb.cnrs-mrs.fr.

which blocks the voltage-gated potassium channel Kv4.2 in a voltage-dependent manner. We demonstrate that this peptide is organized around the ICK structural motif and that it presents a strong electrostatic anisotropy, allowing us to propose a solvent-exposed surface, rich in basic residues and aromatic side chains as being the functional surface of HpTX2.

## Results

### *Preparation and pharmacological characterization of HpTX2*

The yield of fusion protein was ~60 mg/L of culture and the final yield of recombinant HpTX2 was ~1.2 mg/L of culture. The amino acid composition and sequence of the recombinant HpTX2 are identical to the native (data not shown). The molecular mass determined by mass spectrometry was 3,412.7 Da for the recombinant and the native toxin (data not shown). Both peptides presented identical behavior on C18 column and were eluted with a retention time of 34 min (Fig. 1A,B). In conclusion, the recombinant and the native toxin are chemically undistinguishable.

### *Electrophysiology*

The activity of recombinant HpTX2 was examined by the block of Kv4.2 (Sanguinetti et al., 1997). Recombinant HpTX2 at a concentration of 30 nM efficiently blocked the transient outward current elicited in CHO cell, which stably expressed Kv4.2 (75 ± 19% inhibition at −10 mV and ~54 ± 10% inhibition at +40mV, $n = 3$ cells) (Fig. 1C). Inhibition of Kv4.2 channels by the toxin was

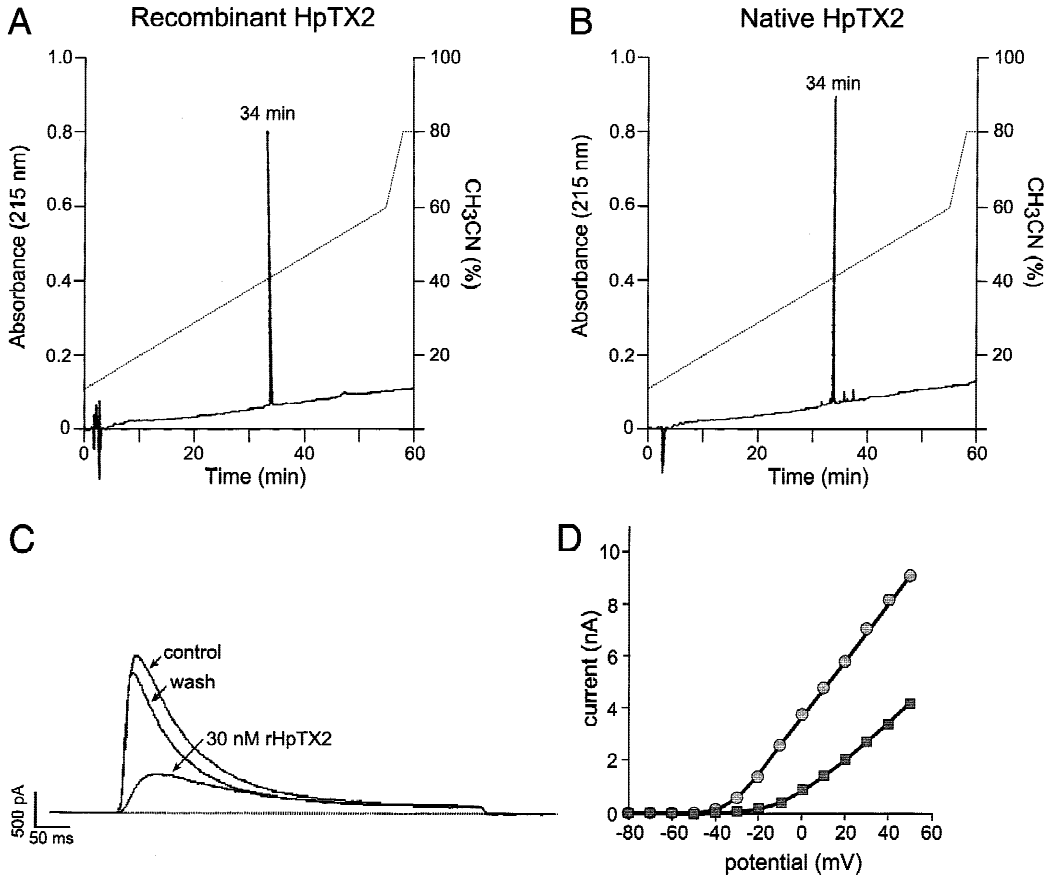


**Fig. 1.** Preparation and pharmacological characterization of HpTX2. **A, B:** Chromatographic profiles of recombinant HpTX2 compared to the native HpTX2. Reverse phase chromatography of purified rHpTX2 (**A**) by exclusion chromatography (see Materials and methods), and (**B**) native HpTX2. One nmole of peptide was loaded on C18 column equilibrated with 0.1% trifluoroacetic acid (TFA), 5% acetonitrile, and eluted with a linear gradient of 5 to 60% in 55 min (vol/vol) with acetonitrile with 0.1% TFA with a second gradient 60–80% with acetonitrile with 0.1% TFA in 3 min. The percentage of acetonitrile ($CH_3CN$) is indicated on the right axis. The flow rate was 1 mL/min, and the absorbance was monitored at 215 nm (left axis). Recombinant and native HpTX2 presented the same high-performance liquid chromatography mobility with a retention time of 34 min in the conditions described above. **C, D:** Effect of recombinant HpTX2 on Kv4.2. Kv4.2 currents were recorded in the whole-cell configuration in CHO cell stably transfected. Holding potential: −80 mV. **C:** Effect of 30 nM recombinant HpTX2 on Kv4.2, recorded at −10 mV with a depolarizing pulse of 500 ms duration. Current traces are shown in the absence (control), in the presence of 30 nM of recombinant HpTX2 and after wash (wash). **D:** The current-voltage relationship for Kv4.2 is shown in the absence (circles) or in the presence of the toxin (squares). The cells were depolarized from a holding potential of −80 mV in increments of 10 mV for 500 ms to potentials between −70 and +60 mV. To investigate the effects of HpTX2, the cells were depolarized from a holding potential of −80 mV to −10 mV for 500 ms. The peaks of the outward currents were analyzed. The stimulation frequency was 0.1 Hz, sample interval was 1 kHz, and the current traces were filter with a frequency of 200 Hz.


**Fig. 2.** Sequence of HpTX2 and sequential assignment. Collected sequential NOEs are classified into strong and weak NOE, and are indicated by thick and thin bars, respectively.

almost totally reversed after wash out (~90% recovery). Current-voltage relations showed that the higher the voltage is, the lower the intensity of blockage (Fig. 1D). This voltage dependence has been described previously (Sanguinetti et al., 1997). These data showed that the recombinant HpTX2 is a powerful inhibitor of the fast inactivating outward K+ current through Kv4.2 channel. In conclusion, the similarities in chemical and blocking properties of recombinant and native HpTX2 indicate the structural identity of both peptides.

*NMR resonance assignment*

Sequential assignment was obtained by the now standard method first described by Wüthrich (1986) and successfully applied to various animal toxins. At the end of the sequential assignment procedure (Fig. 2), almost all protons were identified and their resonance frequency determined.

*Structure calculation*

The structure of HpTX2 was determined by using 218 nuclear Overhauser effect (NOE)-based distance restraints, including 109 intraresidue restraints, 68 sequential restraints, 13 medium-range restraints, and 28 long-range restraints. The repartition of these NOE along the sequence is shown on Figure 3. In addition, 10 hydrogen bond restraints and 19 dihedral angle constraints derived from coupling constants have been included, as well as nine distance restraints derived from the three disulfide bridges. Altogether, the final experimental set corresponded to 8.6 constraints per residue on the average. The structures were calculated by using distance geometry protocol using DIANA and energy minimized by CNS. The best-fit superimposition of backbone atoms for 25 models gives root-mean-square deviation (RMSD) values of 0.63 Å for backbone atoms and 1.12 Å if all nonhydrogen atoms are included (Table 1). Analysis of local RMSD values is summarized on Figure 3 and shows that the precision of the calculation is fairly constant all along the sequence. A summary of the structural statistics is given in Table 1. All the solutions have good nonbonded contacts, and good covalent geometry as evidenced by low values of CNS energy terms and low RMSD values for bond lengths, valence angles, and improper dihedral angles. The correlation with the experimental data shows no NOE-derived distance violation >0.2 Å. The analysis of the Ramachandran plot shows (in PROCHECK software nomenclature) 90.7% of the residues in the most favored and in the additional regions, 6.6% in the generously

**Table 1.** *Structural statistics of the 25 best structures*

| | ⟨DG⟩[a] | ⟨DG⟩[b] |
|---|---|---|
| RMSD (Å) | | |
| Backbone | 0.63 | |
| All heavy atoms | 1.18 | |
| Energies (kcal/mol) | | |
| Total | 102.65 | 110.85 |
| Bonds | 4.96 | 5.00 |
| Angles | 34.96 | 34.59 |
| Impropers | 4.89 | 4.82 |
| van der Waals (repel) | 33.16 | 33.16 |
| NOE | 31.95 | 31.99 |
| cdih | 1.22 | 1.30 |
| RMSD | | |
| Bonds | 0.0033 | 0.0033 |
| Angles | 0.5354 | 0.5332 |
| Dihedral | 32.381 | 32.587 |
| NOE | 0.042 | 0.042 |

[a] ⟨DG⟩ are the final 25 HpTx2 structures obtained by distance geometry and minimization.

[b] ⟨DG⟩ is the minimized mean structure obtained by averaging the coordinates of the individual DG structures best fitted to each other.

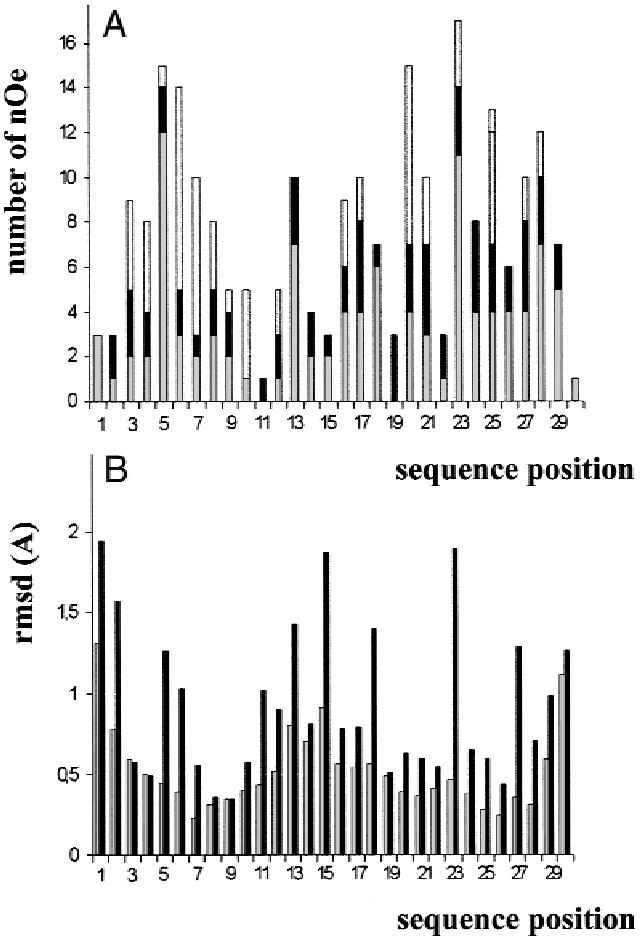


**Fig. 3.** (**A**) NOE and (**B**) RMSD distribution vs. sequence. Intraresidue NOEs are in dark grey; sequential NOEs are in black; medium NOEs are in light grey and long-range NOEs are in white. RMSD value for backbone atoms and all heavy atoms are in grey and black, respectively.

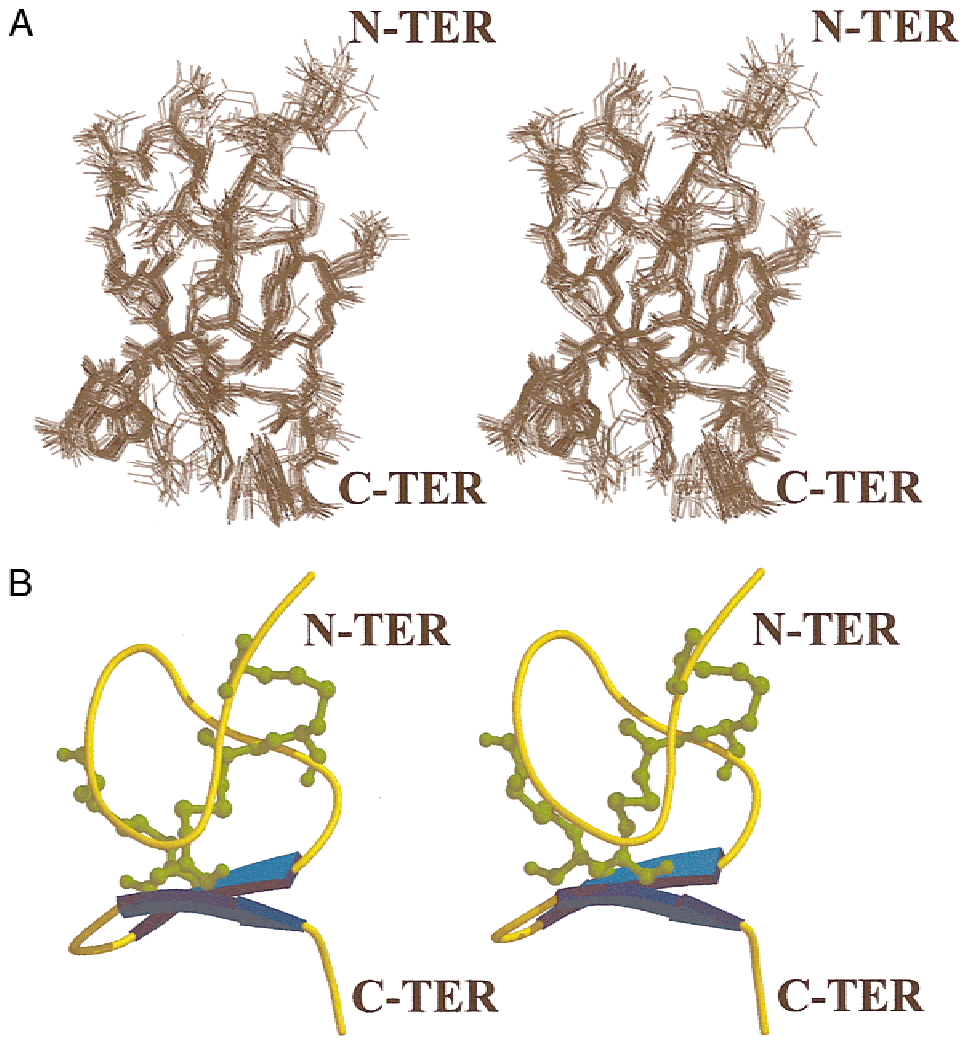


**Fig. 4. A:** Stereoview of the best fit of 25 solution structures of HpTX2. All nonhydrogen atoms are shown. **B:** MOLSCRIPT stereo representation.

allowed regions, and only 2.6% in the disallowed regions (data not shown).

*Structure description*

The 3D structure of HpTX2 (Protein Data Bank id: 1EMX) consists in a compact disulfide-bonded core, from which four loops (4–7, 11–15, 18–21, and 23–25) emerge as well as N- and C-terminii (Fig. 4). The existence of H$\alpha$20–H$\alpha$28 and HN21–HN27 NOE together with an upfield shift of $\alpha$-protons associated with mainly large H$\alpha$–HN coupling constants and slowly exchanged HN proton for residues 21 and 23 is indicative of a short antiparallel $\beta$-sheet encompassing residues 20–23 and 25–28. No other regular secondary structure can be described.

Over the 30 residues of HpTX2, only the side chains of Cys residues are buried. All side-chain conformations are well determined with the exception of Asp1 and Asp2. Analysis of the overall distribution of electrostatic charges reveals a marked anisotropy along the longitudinal axis of the molecule (Fig. 5). The resulting dipole moment of HpTX2 emerges through K27 and is elongated along the main axis. Surrounding K27 are four aromatic residues (W20, W25, W30, and F7), two basic residues (R23 and K25), and three aliphatic residues (L28, L6, and V21). The opposite surface is mainly acidic (D1, D2, D11, E18).

## Discussion

*Comparison with other ion channel inhibitors*

Spider venoms contain a variety of toxic components. The polypeptide toxins are divided into low and high molecular mass types. Low molecular mass polypeptides interact with Ca++, Na+, or K+ channels (for a review, see Grishin, 1999). Hitherto known low molecular mass spider toxins, but also conotoxins from *Conus geographicus* and maurocalcin from the scorpion *Scorpio maurus* share the same ICK structural motif despite their difference in specificity (Fig. 6). As a matter of fact, maurocalcin has been shown to interact with the ryanodin receptor, whereas $\mu$-conotoxin GIIIA is active on muscle sodium channel (Wakamatsu et al., 1992) as well as conotoxin GS (Hill et al.,

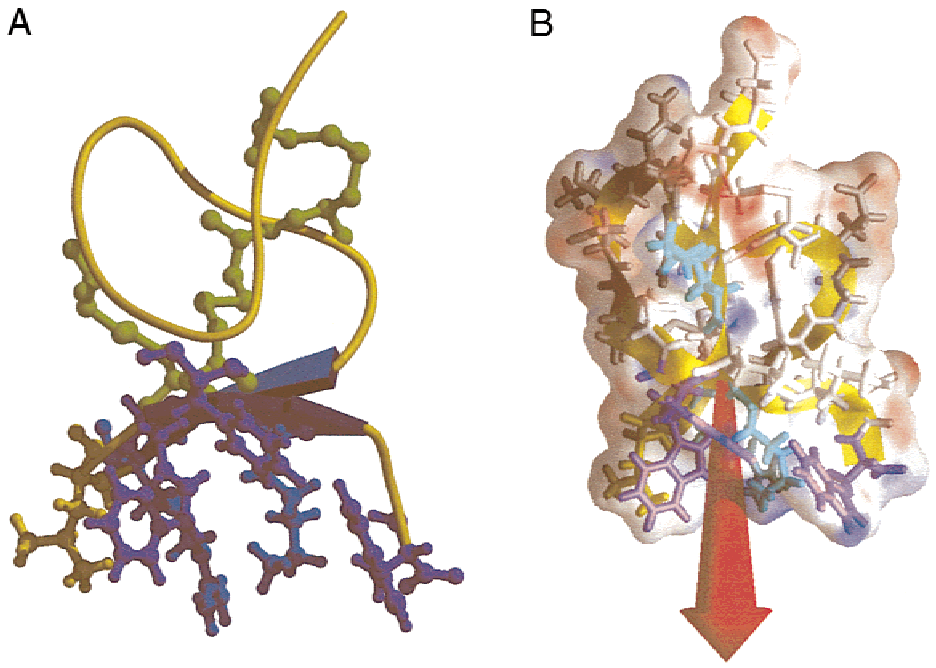


**Fig. 5. A:** MOLSCRIPT representation of the molecule; the side chains of the cystine residues (green) and the ones (purple for aromatic side chains, blue for basic ones and yellow for the aliphatic one) of the putative functional surface are displayed. **B:** Molecular surface colored according to the electrostatic charge (red for acidic and blue for basic) and the resulting dipolar moment (arrow).

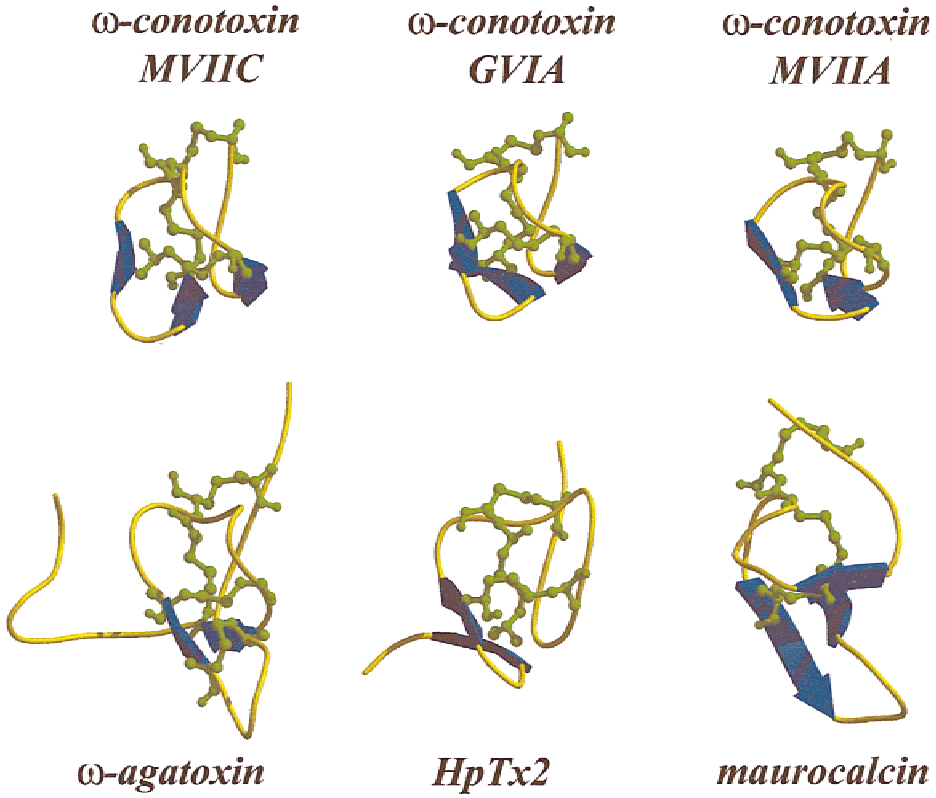


**Fig. 6.** Comparison of 3D structures of structurally related toxins with HpTX2 in MOLSCRIPT representation.

1997) and $\mu$-agatoxin I. By contrast, $\kappa$-conotoxin PVIIA is specific for a voltage-gated potassium channel (Scanlon et al., 1997). Other ICK-toxins have been reported to act on calcium channels: $\omega$-conotoxins MVIIA, MVIIC, GVIA, and GXIA from *C. geographus* (Civera et al., 1999 and references herein) and $\omega$-agatoxin IVA (Kim et al., 1995) from funnel web spider. It seems therefore impossible to guess the specificity of a given toxin by only referring to its 3D structure.

### *Functional surface of HpTX2 and comparison with k-conotoxin PVIIA*

More informative is the analysis of its putative functional surface. In that aim, we have developed a prediction method using the orientation of the dipole moment resulting from the electrostatic anisotropy of the studied toxin as a guideline to predict the functional surface.

Two protruding basic residues (a lysine that is supposed to behave like a tethered K+ ion and to dock into the pore region, an arginine on the edge of the functional surface), an asparagine, a methionine/isoleucine, and an aromatic residue are found in all the potassium channel inhibitor functional sites (Renisio et al., 1999, 2000) and can be considered as the signature motif for their inhibitors. Figure 7 describes the putative functional surface as proposed by the dipole moment orientation. Interestingly, the orientation of the dipole moment of HpTX2 emerges through K27 that could therefore be the critical lysine residue. Close to this lysine are a second basic residue, R23, an aromatic cluster (F7, W25, W30), and a hydrophobic side chain (L24). An additional basic residue K5 is located on the edge of the putative functional surface. The overall physicochemical characteristics of the proposed functional surface of HpTX2 are therefore in good accordance with those of Kv channels inhibitors. They block potassium conductance by physically occluding the extracellular entryway of the pore. Only the asparagine is lacking. Contrarily, $\kappa$-conotoxin PVIIA has been proposed to bind in a voltage-sensitive manner to the external vestibule and to prevent the K+ efflux by steric hindrance (Scanlon et al., 1997; Savarin et al., 1998). In addition, despite poor identity in amino acid sequence, $\kappa$-conotoxin PVIIA and HpTX2 share structural homologies as organized around the same ICK structural motif. Two different proposals have been made concerning the key basic residue that should plug into the pore of the Kv channel: K19 (Scanlon et al., 1997) or K7 (Savarin et al., 1998). When calculating the dipole moment of $\kappa$-conotoxin PVIIA, we found it emerging through K25, which is therefore a third proposal for the crucial basic residue. The corresponding functional surface is shown on Figure 7 in which the central residue is K25 surrounded by K7 on one edge and R18 on the other edge, and by N5, V27, and F23. In such an orientation, we thus get the triplet (K25, N5, and V27 taking place of the isoleucine) and the doublet (F23 and R18 or F23 and K7). Therefore, $\kappa$-conotoxin PVIIA and HpTX2 display the same needed residues in the needed orientation as charybdotoxin (Stampe et al., 1994) to bind to the voltage-activated potassium channels. This may suggest that HpTX2 similarly docks to

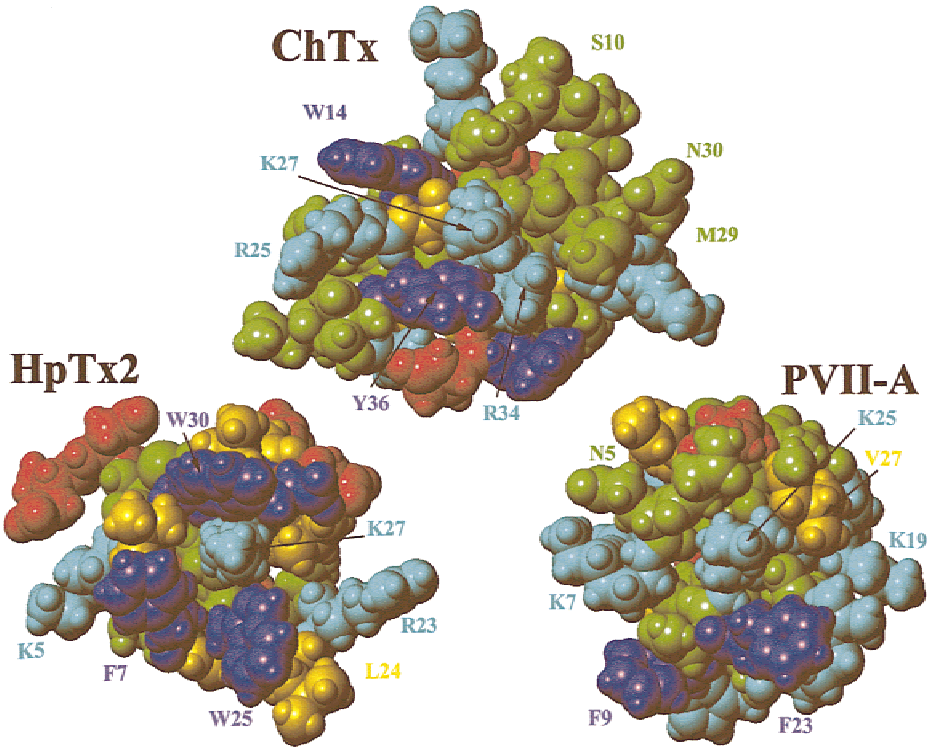


**Fig. 7.** Comparison of the functional surface of charybdotoxin (top) with the ones proposed for k-conotoxin PVIIA (bottom right) and HpTX2 (bottom left). The residues involved (ChTX) or suspected to be involved (PVII-A and HpTX2) are labeled. Residues are colored as follow: green for polar uncharged residues, blue for basic residues, red for acidic residues, purple for aromatic residues, and yellow for aliphatic residues.

the pore region of Kv4.2 channels. The fact that the block of Kv4.2 channels by HpTX2 is voltage-dependent does not contradict this observation. Unlike *Shaker*-related Kv channels, Kv4.2 channels inactivate mainly from a closed state. This gating behavior would be well correlated with the voltage dependence of channel block by HpTX2. Alternatively, HpTX2 may bind to Kv4.2 channels at other surface sites away from the pore entrance. It has been reported that hanatoxin interacts with surface sites of Kv2.1 channels that are 10–15 Å away from the pore axis (Swartz & MacKinnon, 1997). The binding region has been mapped on a region spanning from S3 through S4 segments of the K+ channel, although other regions besides this linker could contribute to the toxin binding site. However, HpTX2 and hanatoxin share only 20% homology excluding the disulfide bridges. Blocking of Kv4.2 induced by HpTX2 by physically occluding the entryway of the pore channel could therefore not be excluded. Unfortunately, the 3D structure of hanatoxin remains so-far unknown, and we therefore cannot check for its dipole orientation.

To ensure the reality of the proposed functional surface and to determine the reason of the specificity of HpTX2 toward Kv4.2 channel (a highly speculative explanation could be the high density in aromatic side chains of the putative functional surface as well as the lack of an asparagine), mutants of HpTX2 are on the way to be produced in which the nature of suspected amino acids to be crucial for binding will be changed.

## Materials and methods

### *Sample preparation*

*Escherichia coli* Xl-1 blue (Stratagene, La Jolla, California) was used for plasmid propagation and for the expression of the MPB2-HpTX2 gene. The pMAL-p2 vector (Biolabs, Frankfurt, Germany) was used for expression of fusion proteins exported in the periplasm (Riggs, 1990).

#### *Synthesis and construction of a HpTX2 gene*

A DNA sequence encoding HpTX2 was constructed by polymerase chain reaction (PCR) using four 36 mers overlapping oligonucleotides. The 107 bp resulting fragment, flanked by a *Hin*dIII site at its 3′ extremity, was inserted into pMAL-p2 between *Xmn*I and *Hin*dIII. After subcloning, the sequence of the construct pMAL-p2HpTX2 was verified by DNA sequencing on both strands.

#### *Expression and purification of the recombinant HpTX2*

*Escherichia coli* Xl-1 blue containing pMAL-p2HpTX2 construct were grown at 37 °C in 8 L of SB medium in the presence of 100 $\mu$g/mL of ampicillin in a fermentor (Biostat B). The expression was induced by adding 0.4 mM IPTG in the mid-logarithmic phase during 3 h. The periplasmic fraction, prepared as described previously (Riggs, 1990), was concentrated and desalted using a 30 K Centricon Plus-80 centrifugal filter (Millipore, Bedford, Massachusetts). Fusion protein was purified by exclusion chromatography on a HighLoad 16/60 Superdex 200 column (Pharmacia, Uppsala, Sweden) using a running buffer containing 20 mM Tris, 100 mM NaCl, pH 8. After concentration (final concentration of ~4 mg/mL), using a centricon 30 K unit (Pallfiltron, Rossdorf, Germany) and addition of 2 mM $CaCl_2$, the cleavage of the MBP2-HpTX2 by factor Xa (1:40, W:W) (Biolabs) was achieved at room temperature for 90 h. The recombinant was purified on a 16/40 Superdex 75 column (Pharmacia) and on a sephasil peptide C18 (Pharmacia, 4.6 × 250 mm, 5 $\mu$m). Native HpTX2 (NPS Pharmaceuticals, Salt Lake City, Utah) was used to compare chromatographic profiles of recombinant and native toxins.

### *Electrophysiology*

Electrophysiological measurements were carried out on CHO cell line which stably expressed (h)Kv4.2 (Zhu et al., 1999) using the whole-cell configuration (Hamill et al., 1981). The cells were perfused with a solution containing 140 mM NaCl, 5 mM KCl, 1 mM MgCl2, 2 mM CaCl2, and 10 mM HEPES, 5 mM glucose, pH 7.3. The micropipettes were filled with 130 mM KCl, 5 mM BAPTA-K4, 10 mM HEPES, 1 mM MgCl2, and 3 mM ATP-Na2, 5 mM glucose, pH 7.2. Bovine serum albumin at 0.05% was added to all HpTX2 containing solutions to prevent nonspecific binding of the toxin. Whole-cell experiments were carried out by means of the patch-clamp technique and performed in the voltage-clamp mode. Experiments were performed at room temperature (23 ± 1 °C). Toxin solution was applied directly to the cells using a fast application system (DAD-12, Adams and List).

### *NMR experiments*

A 1.5 mM sample of HpTx2 in 0.5 mL of $H_2O/D_2O$ (90/10 by vol) at pH 3.0 uncorrected for isotope effects was used for NMR spectra recordings. Amide proton exchange rate was determined after lyophilization of this sample and dissolution in 100% $D_2O$. All $^1H$ NMR spectra were recorded on BRUKER DRX500 spectrometer equipped with a HCN probe and self-shielded triple axis gradients were used. The experiments were performed at 300 K. Two-dimensional spectra were acquired using states-TPPI method (Marion et al., 1989) to achieve F1 quadrature detection (Marion & Wüthrich, 1983). Water suppression was achieved using presaturation during the relaxation delay (1.5 s), and during the mixing time in the case of NOE spectroscopy (NOESY) (Kumar et al., 1981) experiments, or using a watergate 3-9-19 pulse train (Piotto et al., 1992; Sklenar et al., 1992) using a gradient at the magic angle obtained by applying simultaneous *x*-, *y*-, and *z*-gradients prior to detection. NOESY spectra were acquired using mixing times of 80 and 120 ms. Total correlation spectroscopy (TOCSY) (Bax & Davis, 1995; Griesinger et al., 1988) was performed with a spin locking field strength of 8 kHz and mixing time of 80 ms. The amide proton exchange experiments were recorded immediately after dissolution of the peptides in $D_2O$. A series of NOESY spectra with a mixing time of 80 ms were recorded at 300 K, the first one for 1 h, followed by spectra of 10 h each.

#### *Analysis of spectra*

The identification of amino acid spin systems and the sequential assignment were done using the standard strategy described by Wüthrich (1986), applied with a graphical software, XEASY (Bartels et al., 1995). The comparative analysis of correlation spectroscopy and TOCSY spectra recorded in water gave the spin system signatures of the protein. The spin systems were then sequentially connected using the NOESY spectra.

#### *Experimental restraints*

The integration of NOE data was done by measuring the peaks volumes. These volumes were then translated into upper limits

distances by the CALIBA routine of DIANA software (Guntert & Wüthrich, 1991). The lower limit was systematically set at 0.18 nm.

The $\phi$ torsion angles constraints resulted from the $^3J_{\text{HN-H}\alpha}$ coupling constant measurements. They were estimated by the INFIT program (Szyperski et al., 1992). For a given residue, separated NOESY cross peaks with the backbone amide proton in the $\varpi 2$ dimension were used. Several cross sections through these cross peaks were selected that exhibit a good signal-to-noise ratio. They were added up and only those data points of the peak region that were above the noise level were retained. The left and the right ends of the peak region were then brought to zero intensity by a linear baseline correction. After extending the baseline-corrected peak region with zeros on both sides, which is equivalent to over sampling in the time domain, an inverse Fourier transformation was performed. The value of the $^3J_{\text{HN-H}\alpha}$ coupling constant was obtained from the first local minimum. $^3J_{\text{HN-H}\alpha}$ coupling constants were translated into angle restraints using HABAS from the DIANA package.

### *Structure calculation*

Distance geometry calculations were performed with the variable target function program DIANA 2.8. A preliminary set of 1,000 structures was initiated including only intraresidual and sequential upper limit distances. From these, the 500 best were kept for a second round, including medium-range distances, and the resulting 250 best for a third one, with the whole set of upper limits restraints, and some additional distance restraints, used to define the disulfide bridges (i.e., $d_{S\gamma,S\gamma}$ 0.21 nm, $d_{C\beta,S\gamma}$, and $d_{S\gamma,C\beta}$ 0.31 nm). Starting from the 50 best structures, a REDAC strategy (Guntert & Wüthrich, 1991) was used in a last step to include the dihedral constraints together with the additional distances restraints coming from hydrogen bonds.

To remove residual bad Van der Waals contacts, these 50 structures were refined by restrained molecular dynamics annealing, slow cooling, and energy minimization (parameter file: protein-allhdg in CNS).

The visual analysis were done using the TURBO software and the geometric quality of the obtained structures was assessed by PROCHECK 3.3 and PROCHECK-NMR softwares (Laskowski et al., 1993).

## Acknowledgments

The authors would like to thank Stephane Canarelli for amino acid analysis and sequence determination, Christian Schulze for technical assistance, Olivier Bornet for NMR spectra acquisitions, and Christian Cambillau for constant help and support. We also thank NPS Pharmaceuticals for the generous gift of natural HpTX2 molecule.

## References

Aiyar J, Rizzi JP, Gutman GA, Chandy KG. 1996. The signature sequence of voltage-gated potassium channels projects into the external vestibule. *J Biol Chem 271*:31013–31016.

Bartels Ch, Xia T-H, Billeter M, Güntert P, Wüthrich K. 1995 The program XEASY for computer-supported NMR spectral analysis of biological macromolecules. *J Biomol NMR 5*:1–10.

Bax A, Davis DG. 1995. MLEV-17-based two-dimensional homonuclear magnetization transfer spectroscopy. *J Magn Reson 65*:355–360.

Blanc E, Lecomte C, Van Rietschoten J, Sabatier JM, Darbon H. 1997. Solution structure of Tskapa, a charybdotoxin-like scorpion toxin from *Tityus serrulatus* with high affinity for apamin-sensitive Ca2+-activated K+ channel. *Proteins 29*:359–369.

Bystrov VF, Okhanov VV, Miroshnikov AI, Ovchinnikov YA. 1980. Solution spatial structure of apamin as derived from NMR study. *FEBS Lett 119*: 113–117.

Civera C, Vazquez A, Sevilla JM, Bruix M, Gago F, Garcia AG, Sevilla P. 1999. Solution structure determination by 2D $^1$H NMR of $\omega$-conotoxin TIVIID, a calcium channel blocker peptide. *Biochem Biophys Res Com 254*:32–35.

Darbon H, Blanc E, Sabatier J-M. 2000. 3D structure of scorpion toxin: Towards a new model of interaction with potassium channel. In: Darbon H, Sabatier J-M, eds. *Perspective in drug discovery and design, vols. 15/16*. Dordrecht: Kluwer. pp 41–60.

Flinn JP, Pallaghy PK, Lew MJ, Murphy R, Angus JA, Norton RS. 1999. Roles of key functional groups in w-conotoxin GVIA. *Eur J Biochem 262*:447–455.

Fremont V, Blanc E, Crest M, Eauclaire MF, Gola M, Darbon H, Van Rietschoten J. 1997. Dipole moments of scorpion toxins direct the interaction towards small- or large-conductance $Ca^{++}$-activated $K^+$ channels. *Lett Peptide Sci 4*:305–312.

Goldstein SAN, Pheasant DJ, Miller C. 1994. The charybdotoxin receptor of a shaker K+ channel: Peptide and channel residues mediating molecular recognition. *Neuron 12*:1377–1388.

Griesinger C, Otting G, Wüthrich K, Ernst RR. 1988. Clean-TOCSY for 1H spin system identification in macromolecules. *J Am Chem Soc 110*:7870–7872.

Grishin E. 1999. Polypeptide neurotoxins from spider venoms. 1999. *Eur J Biochem 264*:276–280.

Guntert P, Wüthrich K. 1991. Improved efficiency of protein structure calculations from NMR data using the program DIANA with redundant dihedral angle constraints. *J Biomol NMR 1*:447–456.

Habermann E, Fischer K. 1979. Apamin, a centrally acting neurotoxic peptide: Binding and actions. *Adv Cytopharmacol 3*:387–394.

Hamill OP, Marty A, Neher E, Sakmann B, Sigworth FJ. 1981. Improved patch-clamp techniques for high-resolution current recording from cells and cell-free membrane patches. *Pflugers Arch 391*:85–100

Hill JM, Alewood PF, Craik DJ. 1997. Solution structure of the sodium channel antagonist conotoxin GS: A new molecular caliper for probing sodium channel geometry. *Structure 5*:571–583

Kim JI, Konishi S, Iwai H, Kohno T, Gouda H, Shimada H, Sato K, Arata Y. 1995. 3D solution structure of the calcium channel antagonist co-agatoxin IVA: Consensus molecular folding of calcium channel blockers. *J Mol Biol 250*:659–671.

Kumar A, Ernst RR, Wüthrich K. 1981. A two-dimensional nuclear Overhauser enhancement (2D NOE) experiment for the elucidation of complete proton-proton cross-relaxation networks in biological macromolecules. *Biochem Biophys Res Commun 95*:1–6.

Laskowski RA, MacArthur MW, Moss DM, Thornton JM. 1993. A program to check the stereochemical quality of protein structures. *J Appl Crystallogr 26*:283–291.

Marion D, Ikuto Tschudin M, Bax A. 1989. Rapid recording of 2D NMR spectra without phase cycling. Application to the study of hydrogen exchange in protein. *J Mag Reson 85*:393–399.

Marion D, Wüthrich K. 1983. Application of phase sensitive two dimensional correlated spectroscopy (COSY) for measurements of H-H spin-spin coupling constants in proteins. *Biochem Biophys Res Commun 113*:967–974.

Miller C. 1995.The charybdotoxin family of K+ channel-blocking peptides. *Neuron 15*:5–10

Naranjo D, Miller C. 1996. A strongly interacting pair of residues on the contact surface charybdotoxin and a shaker channel. *Neuron 16*:123–130.

Pease JH, Wemmer DE. 1988. Solution structure of apamin determined by nuclear magnetic resonance and distance geometry. *Biochemistry 27*:8491–8498.

Piotto M, Saudek V, Sklenar V. 1992. Gradient-tailored excitation for single-quantum NMR spectroscopy of aqueous solutions. *J Biomol NMR 2*:661–665

Possani LD. 1984. Insect poisons, allergens, and other invertebrate venoms. In: Tu E, ed. *Handbook of natural toxins*, vol. 2. New York: Marcel Deckker. pp 607–636

Rangananthan R, Lewis JH, MacKinnon R. 1996. Spatial localization of the $K^+$ channel selectivity filter by mutant cycle-based structure analysis. *Neuron 16*:131–139.

Renisio JG, Lu Z, Blanc E, Jin W, Lewis JH, Bornet O, Darbon H. 1999. Solution structure of potassium channel-inhibiting scorpion toxin Lq2. *Proteins 34*:417–426

Renisio JG, Romi-Lebrun R, Blanc E, Bornet O, Nakajima T, Darbon H. 2000. Solution structure of BmKTX, a K+ blocker toxin from the Chinese scorpion *Buthus martensi*. *Proteins 38*:70–78.

Riggs P. 1990. Purification of fusion proteins from the periplasm. In: Ausebel FM, eds. *Current protocols in molecular biology*. New York: Greene Associates/Wiley Interscience.

Sanguinetti MC, Johnson JH, Hammerland LG, Kelbaugh PR, Volkmann RA, Saccomano NA, Mueller AL. 1997. Heteropodatoxins: Peptides isolated

from spider venom that block Kv4.2 potassium channels. *Mol Pharmacol 51*:491–498.

Savarin P, Guenneugues M, Gilquin B, Lamthanh H, Gasparini S, Zinn-Justin S, Menez A. 1998. Three-dimensional structure of kappa-conotoxin PVIIA, a novel potassium channel-blocking toxin from cone snails. *Biochemistry 37*:5407–5416.

Scanlon MJ, Naranjo D, Thomas LA, Alewood PF, Lewis RJ, Craik DJ. 1997. Solution structure and proposed binding mechanism of a novel potassium channel toxin k-conotoxin PVIIA. *Structure 5*:1585–1597.

Sklenar V, Piotto M, Leppik R, Saudek V. 1992. Gradient-tailored water suppression for 1H-15N HSQC experiments optimised to retain full sensitivity. *J Mag Reson 102*:241–245.

Stampe P, Kolmakova-Partenski L, Miller C. 1994. Intimation pf K+ channel from a complete functional map of the molecular surface of charybdotoxin. *Biochemistry 33*:443–450.

Swartz KJ, MacKinnon R. 1997. Hanatoxin modifies the gating of a voltage-dependent K+ channel through multiple binding sites. *Neuron 18(4)*:665–673.

Szyperski T, Güntert P, Otting G, Wüthrich K. 1992. Determination of scalar coupling constants by inverse Fourier transformation of in-phase multiplets. *J Magn Reson 99*:552–560.

Vincent JP, Schweitz H, Lazdunski M. 1975. Structure-function relationships and site of action of apamin, a neurotoxic polypeptide of bee venom with an action on the central nervous system. *Biochemistry 14*:2521–2525.

Wakamatsu K, Kohda D, Hatanaka H, Lancelin JM, Ishida Y, Oya M, Nakamaru H, Inagaki F, Sato K. 1992. Structure-activity relationships of $\mu$-conotoxin GIIIA: Structure determination of active and inactive sodium channel blocker peptides by NMR and simulated annealing calculations. *Biochemistry 31*:12577–12584.

Wüthrich K. 1986. Resonance assignment and structure determination in proteins. In: *NMR of proteins and nucleic acids*. New York: John Wiley and Sons.

Zhu XR, Wulf A, Schwarz M, Isbrandt D, Pongs O. 1999. Characterization of human Kv4.2 mediating a rapidly-inactivating transient voltage sensitive K+ current. *Receptors Channels 6*:387–400.